Proceedings of the
47th IEEE Conference on Decision and Control
Cancun, Mexico, Dec. 9-11, 2008

A Locally Most Powerful Detector for Mode Perturbation Signatures

Paul G. Otanez
paul.otanez@gm.com
Powertrain Systems Research Lab
General Motors Research & Development

Mark E. Campbell
mc288@cornell.edu
Deparmtnet of Mechanical & Aerospace Engineering
Cornell University

***Abstract*—A new method to enable vehicle mode detection in a cooperative environment while minimizing communication is proposed. The behavior of a vehicle is described using a finite number of operating modes. Each mode is defined by a model which describes the vehicle's dynamics as well as a perturbation signature based on Gold codes. To accomplish mode detection a locally most powerful detector is derived in which the test statistic is evaluated using the Kalman Filter innovations. The performance of the locally most powerful detector is tested via Monte Carlo simulations of a linear and a nonlinear system.**

I. Introduction

Cooperative control approaches, such as those addressed in Refs. [1] and [2], have been shown to work well in a variety of missions such as cooperative reconnaissance and coordinated strikes. "Swarms" of small versions of these vehicles are now being envisioned because of the ability to build strong, robust small scale electronics and smart sensors, economies of scale, and robustness that accompanies large numbers. Implementation of swarms, or "active networks" is non-trivial, and involves a coordinated effort to address control, sensing of the environment, distributed and collaborative processing, and decision making [3], [4], [5], [6]. Cooperative control algorithms for these teams of vehicles acting in the presence of a communication network must be robust to communication failures, outages, or blackouts, and must also scale well with the numbers of vehicles. The work here focuses on a non-traditional approach of enabling inter-vehicle communications for the problem of cooperative control, where partner vehicles are considered part of the environment. The goal is to improve collaborative performance using minimal communications. Applications where this work would be enabling include: 1) stealth like missions, where communications are forbidden, 2) multi-vehicle systems where communications are "expensive" (i.e. power), such that short broadcasts or multi-hop are required, 3) multi-vehicle networked systems where faults have occurred, and 4) active sensor networks with actions that are decided locally, but global behavior is desired.

More specifically, this paper investigates the problem of locally estimating (on each vehicle) the behavior of the environment, with specific focus on partner vehicles, in order to improve performance and decision making. Partner vehicles are described with behaviors defined by a finite number of operating modes. Each mode of the system not only includes a model that describes the vehicle's dynamics, but also includes a unique motion-based signature based on Gold Codes. For example, in the case of cooperative reconnaissance, the partner vehicle's operating modes could include: 1) search an area, 2) locate a target, and 3) identify a target. Therefore the motion-based signatures are the basis of the non-traditional low-rate communications protocol between aircraft. A locally most powerful detection algorithm is used to determine the current operating mode of each partner vehicle from sensor measurements, thus enabling vehicles to probabilistically know what their partner vehicles are doing even with no communications.

In Ref. [7] a suboptimal mode detection is achieved by estimating the motion of the vehicle and the mode perturbation signature with a Kalman Filter (KF) (the implementation of the suboptimal approach in a reconnaissance problem is presented in Ref. [8]). The resultant estimate is then correlated with a set of mode perturbation signature replicas. In this investigation, an alternative mode detection method is derived which evaluates a Neyman-Pearson locally most powerful hypothesis test statistic using the innovations of the KF. If the amplitude of the mode perturbation signature is assumed to be small, the locally most powerful detector is optimal in terms of minimizing the probability of missed detection for a given probability of false alarm [9].

The paper is presented as follows. Section II describes the logistics of using motion-based signatures to transmit information between vehicles. In Section III, a locally most powerful detector under the presence of Gaussian measurement noise is derived. In Section IV, Monte Carlo methods are used to test the detector's performance on two examples. First, the KF is used on a linear model, and second the Sigma Point Filter (SPF) is used on a two-dimensional model with nonlinear radar-like output equations. Both examples discuss how the model-based estimators are tuned.

II. Mode Estimation Method

The motivation for assigning a unique signature to each of the i modes is to facilitate mode estimation and thus enable the exchange of vehicle information in the absence of a formal communication system. By knowing which mode a partner vehicle is operating in, a higher quality of cooperation can be realized. Figure 1 shows each component of this mode estimation process for a two vehicle system. It should be noted that the method presented here applies to more than two vehicles. The first vehicle transfers information by choosing a corresponding operating mode, i, which is then encoded into a mode perturbation signature, z^i_{sig}. The scalar mode perturbation signature is transformed by the controller into a vehicle perturbed reference, $\mathbf{r}^i_{\text{sig}}$, and combined with the nominal vehicle reference, $\mathbf{r}$, to define the total reference, $\bar{\mathbf{r}}^i$. The controller calculates the total control input $\bar{\mathbf{u}}^i_{\text{sig}}$ as a function of its vehicle state estimate, $\hat{\mathbf{x}}$, and $\bar{\mathbf{r}}^i$. The total control input drives the nonlinear vehicle dynamics, and its response, $\bar{\mathbf{y}}$, is fed into a vehicle state estimator for use by the first vehicle for its controller.

A mode detection method is used on the second vehicle to detect the operating mode of the first vehicle. The mode detector block uses the measurements of the second vehicle's monitoring sensors, denoted as $\mathbf{y}$, and the stored mode perturbation signatures replica, $\tilde{z}^i_{\text{sig}}$, to detect the mode which was transmitted by the first vehicle. The mode estimate, $\hat{i}$, is used by the planner on the second vehicle to modify its behavior.

A. Signature Generation

Consider a rectangular pulse composed of m_ρ points defined at T time intervals and chip duration $T_c = m_\rho T$ or with value ρ^0 or ρ^1 corresponding to the 0 or 1 respectively (other values could be

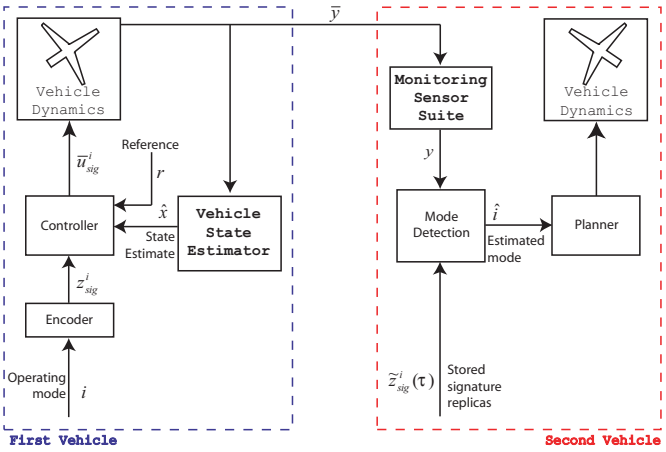

Fig. 1. A block diagram of how information is exchanged via movements between two vehicles.

used). Let the sequence of such n_ρ nonoverlapping rectangular chips (or pulses) for the i^{th} signature be defined as

$$p^i = \left[b_{i,1}, b_{i,2}, \ldots, b_{i,n_\rho}\right] \tag{1}$$

where $p^i \in \mathbb{R}^{n_\rho}$ and $b_{(\cdot)} \in \left[\rho^0, \rho^1\right]$. The i^{th} mode perturbation signature, z^i_{sig}, is formally defined at time k as the product of the chip sequencep^i and a sinusoidal carrier:

$$z^i_{\text{sig},k} = p^i_k \cos\left[2\pi f_c t_k + \theta_k\right], \tag{2}$$

where f_c, the carrier frequency, and θ is the carrier phase. By combining n_ρ chips, a mode signature, z^i_{sig} is defined.

Pseudonrandom noise (PRN) is a known sequence of bits that, when added to a base signal, results in a signal which has statistical properties similar to noise [10]. Gold Codes are a type of PRN sequences that have desirable properties in terms of auto and cross-correlation and therefore are chosen to define the mode signatures in this investigation [11]. Because each mode perturbation signature z^i_{sig} is defined using the observed vehicle's internal time clock, the observing vehicle must use correlation to determine if there a clock offset, τ, with its stored mode signature replica, $\tilde{z}_{\text{sig}}$. The delay, τ, that maximizes the correlation is the estimated clock offset or delay and is denoted as $\hat{\tau}$.

In summary, for a direct-sequence system with phase modulation, the mode perturbation signature with scaling factor a_{sig} received is modeled as:

$$a_{\text{sig},k} z^i_{\text{sig},k} = a_{\text{sig},k} p^i_k[\tau] \cos\left[2\pi f_c t_k + 2\pi f_{d,k} + \theta_k\right], \tag{3}$$

where at time k, p^i_k is the i^{th} spreading waveform (Gold code with $\rho^0 = -1$ and $\rho^1 = 1$ for bipolar-phase shift keying (BPSK)) with phase τ, f_c is the carrier frequency, and θ_k is the random carrier phase. The variables τ and f_d are the code phase delay and carrier frequency offset, respectively, which must be estimated at the receiver. Equation (3) is the signal model that would be used at the vehicle observing (receiving) the mode perturbation signature. The frequency offset, f_d, may be due to a Doppler shift, or to a drift or an instability in the transmitter's oscillator.

B. Controller

Each mode, denoted the i^{th} mode, is correlated with a signature; there are N modes or mode perturbation signatures defined. The approach here is to express the signature using Gold Codes, and then use this signature as an input to the vehicle system dynamics as shown in Figure 1. To begin, consider at time k a nominal reference input signal, $\mathbf{r}_k$, and a small perturbation to the signal, $\mathbf{r}^i_{\text{sig},k}$. The total reference signal with the perturbation, $\bar{\mathbf{r}}^i_k$, is then $\bar{\mathbf{r}}^i_k = \mathbf{r}_k + \mathbf{r}^i_{\text{sig},k}$. In order to express the scalar signature z^i_{sig} in the physical reference coordinates, $\mathbf{r}_k$, let $t^r_z(\cdot)$ denote the mapping from the scalar signature to the reference:

$$\mathbf{r}^i_{\text{sig}} = a_{\text{sig}} t^r_z\left(z^i_{\text{sig}}\right). \tag{4}$$

Finally, a feedback controller which minimizes the tracking is required to assure that the vehicle tracks the desired total reference $\bar{\mathbf{r}}^i_k$. Such controller feedback controller that can be linear, nonlinear, etc., can be expressed as:

$$\bar{\mathbf{u}}^i_k = c\left(\hat{\mathbf{x}}_k, \mathbf{r}_k + \mathbf{r}^i_{\text{sig},k}\right). \tag{5}$$

C. Hybrid Model

The behavior of a vehicle in a team of vehicles is formulated as a hybrid system defined by a finite set of N operating modes. The vehicle dynamics and state evolution for the i^{th} mode are governed by:

$$\mathbf{x}_{k+1} = f^i\left(\mathbf{x}_k, \bar{\mathbf{u}}^i_k, z^i_{\text{sig},k}, \mathbf{w}_k\right), \quad \mathbf{y}_k = h^i\left(\mathbf{x}_k, \bar{\mathbf{u}}^i_k, z^i_{\text{sig},k}, \mathbf{v}_k\right), \tag{6}$$

where at time k, $\mathbf{x}_k \in \mathbb{R}^{n_x}$ is the state, $\mathbf{y}_k \in \mathbb{R}^{n_y}$ the measurement, $\bar{\mathbf{u}}_k \in \mathbb{R}^{n_u}$ the control input from Equation (5), and $z^i_{\text{sig},k} \in \mathbb{R}$ is a scalar signature which represents the i^{th} mode. The process noise $\mathbf{w}_k$ and sensor noise $\mathbf{v}_k$ are zero-mean white Gaussian signals with covariances, $E\left[\mathbf{w}_k \mathbf{w}^T_k\right] = Q_k$, $E\left[\mathbf{v}_k \mathbf{v}^T_k\right] = R_k$.

III. The Locally Most Powerful Mode Detector

In this section an optimal test statistic is derived which is based on detection theory that consists of solely correlating the measured movements of the vehicle with mode perturbation signature replicas. However, it is advantageous to derive an equivalent mode detection test statistic which integrates a model-based estimator used to handle noisy measurements. The results in this section show that the sum of the innovations of the model-based estimator is an equivalent way to evaluate the locally most powerful mode detector.

Consider a signal detection problem which has two hypotheses:

$$H_0 : \mathbf{y} = \mathbf{n}, \tag{7}$$

$$H_1 : \mathbf{y} = a_{\text{sig}} \mathbf{z}^{i,\tau,\theta,f_c}_{\text{sig}} + \mathbf{n}, \tag{8}$$

where $\mathbf{y} \in \mathbb{R}^{n_m}$ is a vector containing n_m scalar measurements and $\mathbf{n} \in \mathbb{R}^{n_m}$ is zero-mean Gaussian noise, with covariance $P \in \mathbb{R}^{n_m \times n_m}$. The variable $\mathbf{z}^{i,\tau,\theta,f_c}_{\text{sig}}$ is a stacked vector of n_m scalar signatures $z^{i,\tau,\theta,f_c}_{\text{sig}}$,

$$\mathbf{z}^{i,\tau,\theta,f_c}_{\text{sig}} = \begin{bmatrix} z^{i,\tau,\theta,f_c}_{\text{sig},1} \\ z^{i,\tau,\theta,f_c}_{\text{sig},2} \\ \vdots \\ z^{i,\tau,\theta,f_c}_{\text{sig},n_m} \end{bmatrix}, \tag{9}$$

where

$$z^{i,\tau,\theta,f_c}_{\text{sig,k}} = p^i_k[\tau] \cos\left[2\pi f_c t_k + \theta_k\right]. \tag{10}$$

Given the measurements $\mathbf{y}$, the hypothesis H_0 represents the belief that there was no signal present, while the hypothesis H_1 represents

the belief that a signal was present. The term $\mathbf{z}_{\text{sig}}^{i,\tau,\theta,f_c} \in \mathbb{R}^{n_m}$ defines the mode perturbation history for the i^{th} mode, as a function of the Gold Code with phase τ, carrier sinusoid phase θ, and carrier frequency f_c. The frequency offset term, f_d, is omitted from $\mathbf{z}_{\text{sig}}^{i,\tau,\theta,f_c}$ without loss of generality. The parameter a_{sig} is the unknown scalar amplitude of the mode perturbation history. The measurement probability density functions, or likelihoods, under both hypotheses are written as:

$$p(\mathbf{y}|H_0) = \frac{1}{2\pi^{\frac{n_m}{2}}|P|^{\frac{1}{2}}} \exp\left[-\frac{1}{2}\mathbf{y}^T P^{-1}\mathbf{y}\right], \quad (11)$$

$$p(\mathbf{y}|H_1) = \frac{1}{2\pi^{\frac{n_m}{2}}|P|^{\frac{1}{2}}} \exp\left[-\frac{1}{2}\left(\mathbf{y}-a_{\text{sig}}\mathbf{z}_{\text{sig}}^{i,\tau,\theta,f_c}\right)^T P^{-1} \left(\mathbf{y}-a_{\text{sig}}\mathbf{z}_{\text{sig}}^{i,\tau,\theta,f_c}\right)\right]. \quad (12)$$

The corresponding Neyman-Pearson hypothesis test statistic [9] for evaluating whether to accept H_1 is then written as a likelihood ratio:

$$\lambda(\mathbf{y}) = \frac{p(\mathbf{y}|H_1)}{p(\mathbf{y}|H_0)} \geq \lambda_{\text{thresh}}, \quad (13)$$

where λ_{thresh} is a threshold that if exceeded, determines whether hypothesis H_1 should be accepted. It is noted that λ_{thresh} can be chosen as to minimize a probability of false alarm.

It is desirable to remove the dependence of $p(\mathbf{y}|H_1)$, Equation (12), on the carrier phase θ, since it would simplify the formulation and reduce the number of computations required in the evaluation of the detection test statistic. A random carrier phase delay θ is assumed in this formulation, and can be modeled as a uniformly distributed random variable from 0 to 2π radians. This represents the belief that all phases are equally likely to occur. The marginal probability density, $p_\theta(\mathbf{y}|H_1)$, for the probability density function, Equation (12), can be computed to remove its dependency on the carrier phase delay. The likelihood ratio is reformulated by substituting $p_\theta(\mathbf{y}|H_1)$ into Equation (13) which results in:

$$\lambda_\theta(\mathbf{y}) = \frac{p_\theta(\mathbf{y}|H_1)}{p(\mathbf{y}|H_0)}. \quad (14)$$

By expanding Equation (14) and then moving the terms corresponding to $p(\mathbf{y}|H_0)$ inside the integral, the Neyman-Pearson hypothesis test statistic can then be simplified to:

$$\lambda_\theta(\mathbf{y}) = c_\lambda \int_0^{2\pi} \exp\left\{a_{\text{sig}}\mathbf{y}^T P^{-1}\mathbf{z}_{\text{sig}}^{i,\tau,\theta,f_c}\cdot\right\} -\frac{1}{2}a_{\text{sig}}^2\left(\mathbf{z}_{\text{sig}}^{i,\tau,\theta,f_c}\right)^T P^{-1}\mathbf{z}_{\text{sig}}^{i,\tau,\theta,f_c}\Big\} d\theta. \quad (15)$$

where $c_\lambda = \frac{1}{2\pi}$.

Because a_{sig} is unknown and must be estimated, a Neyman-Pearson locally most powerful test statistic is then formulated. First, in hypothesis H_1 it is assumed that a_{sig} is known. Equation (15) is used to derive a Neyman-Pearson locally most powerful (LMP) test in the limit of small, but known a_{sig}. The LMP theory shows that this limits minimizes the probability of missed detection for a given probability of false alarm for all small a_{sig} [9]. The LMP test is derived by expanding Equation (15) into a Taylor series around a_{sig} that yields:

$$\lambda_\theta(\mathbf{y}) \approx \lambda_\theta(\mathbf{y})|_{a_{\text{sig}}=0} + \left.\frac{\partial\lambda_\theta(\mathbf{y})}{\partial a_{\text{sig}}}\right|_{a_{\text{sig}}=0} a_{\text{sig}} + \frac{1}{2}\left.\frac{\partial^2\lambda_\theta(\mathbf{y})}{\partial a_{\text{sig}}^2}\right|_{a_{\text{sig}}=0} a_{\text{sig}}^2. \quad (16)$$

The first term in the Taylor series in Equation (16) is a constant defined as c_{λ_0}. Evaluating the second term of the series in Equation (16) requires differentiating Equation (15) with respect to a_{sig}, which after substituting $a_{\text{sig}} = 0$ yields:

$$\left.\frac{\partial\lambda_\theta(\mathbf{y})}{\partial a_{\text{sig}}}\right|_{a_{\text{sig}}=0} = c_\lambda \int_0^{2\pi} \mathbf{y}^T P^{-1}\mathbf{z}_{\text{sig}}^{i,\tau,\theta,f_c} d\theta. \quad (17)$$

In order to compute the integral with respect to θ, it is necessary to expand the expression for the mode perturbation signature, $z_{\text{sig}}^{i,\tau,\theta,f_c}$. At time k, the discrete time version of the mode perturbation signature in Equation (2) has the form:

$$z_{\text{sig},k}^{i,\tau,\theta,f_c} = p_k^i(\tau)\cos[2\pi f_c t_k - \theta_k], \quad (18)$$

where the unknown carrier phase delay, θ_k, is subtracted to simplify the derivation. Using trigonometric identities Equation (18) can be written as:

$$z_{\text{sig},k}^{i,\tau,\theta,f_c} = z_{\cos,k}^{i,\tau,f_c}\cos[\theta_k] + z_{\sin,k}^{i,\tau,f_c}\sin[\theta_k], \quad (19)$$

where $z_{\cos,k}^{i,\tau,f_c} = p_k^i(\tau)\cos[2\pi f_c t_k]$, and $z_{\sin,k}^{i,\tau,f_c} = p_k^i(\tau)\sin[2\pi f_c t_k]$. Substituting Equation (19) into Equation (17) and computing the integral with respect to θ results in $\left.\frac{\partial\lambda(\mathbf{y})}{\partial a_{\text{sig}}}\right|_{a_{\text{sig}}=0} = 0$. Therefore no useful locally most powerful detector is found from the second term since it vanishes for small a_{sig}.

Moving onto the third term in the series, the likelihood ratio, Equation (15), can be differentiated with respect to a_{sig}. The differentiation of Equation (15) twice with respect to a_{sig} and then substituting $a_{\text{sig}} = 0$ yields:

$$\left.\frac{\partial^2\lambda_\theta(\mathbf{y})}{\partial a_{\text{sig}}^2}\right|_{a_{\text{sig}}=0} = c_\lambda \int_0^{2\pi} \Big\{-\left(\mathbf{z}_{\text{sig}}^{i,\tau,\theta,f_c}\right)^T P^{-1}\mathbf{z}_{\text{sig}}^{i,\tau,\theta,f_c} + \left(\mathbf{y}^T P^{-1}\mathbf{z}_{\text{sig}}^{i,\tau,\theta,f_c}\right)^2\Big\} d\theta. \quad (20)$$

For clarity, the terms inside the integrals are computed separately. The first term is derived by realizing that $\left(\mathbf{z}_{\cos}^{i,\tau,f_c}\right)^T P^{-1}\mathbf{z}_{\cos}^{i,\tau,f_c} \approx \left(\mathbf{z}_{\sin}^{i,\tau,f_c}\right)^T P^{-1}\mathbf{z}_{\sin}^{i,\tau,f_c}$ for a diagonal P (uncorrelated noise), and a long time interval, and then computing the integral over θ yielding:

$$-\int_0^{2\pi}\left(\mathbf{z}_{\text{sig}}^{i,\tau,\theta,f_c}\right)^T P^{-1}\mathbf{z}_{\text{sig}}^{i,\tau,\theta,f_c} = c_{z^T P^{-1} z}. \quad (21)$$

The second term is computed by substituting the signature definition in Equation (19) into Equation (20) and computing the integral over θ yielding:

$$\int_0^{2\pi}\left(\mathbf{y}^T P^{-1}\mathbf{z}_{\text{sig}}^{i,\tau,\theta,f_c}\right)^2 d\theta = \pi\left(\mathbf{y}^T P^{-1}\mathbf{z}_{\cos}^{i,\tau,f_c}\right)^2 + \pi\left(\mathbf{y}^T P^{-1}\mathbf{z}_{\sin}^{i,\tau,f_c}\right)^2. \quad (22)$$

Substituting the two terms, Equations (21) and (22), into Equation (20) results in:

$$\left.\frac{\partial^2\lambda_\theta(\mathbf{y})}{\partial a_{\text{sig}}^2}\right|_{a_{\text{sig}}=0} = c_\lambda\left\{c_{z^T P^{-1} z} + \pi\left(\mathbf{y}^T P^{-1}\mathbf{z}_{\cos}^{i,\tau,f_c}\right)^2 + \pi\left(\mathbf{y}^T P^{-1}\mathbf{z}_{\sin}^{i,\tau,f_c}\right)^2\right\}. \quad (23)$$

Finally by substituting Equations (21) and (23) into Equation (16)

results in the following definition of the LMP test statistic:

$$\lambda_{\text{LMP}}(\mathbf{y}) \approx c_{\lambda_0} + \frac{1}{2}c_\lambda \left\{ c_{z^T P^{-1} z} + \pi \left(\mathbf{y}^T P^{-1} \mathbf{z}_{\cos}^{i,\tau,f_c} \right)^2 + \pi \left(\mathbf{y}^T P^{-1} \mathbf{z}_{\sin}^{i,\tau,f_c} \right)^2 \right\} a_{\text{sig}}^2. \quad (24)$$

As stated in Equation (13), $\lambda_{\text{LMP}}(\mathbf{y})$ can be compared to λ_{thresh} to determine the acceptance of hypothesis H_1, or $\lambda_{\text{LMP}} \geq \lambda_{\text{thresh}}$. This inequality after substituting Equation (24) can be manipulated to yield the following:

$$\left(\mathbf{y}^T P^{-1} \mathbf{z}_{\cos}^{i,\tau,f_c} \right)^2 + \left(\mathbf{y}^T P^{-1} \mathbf{z}_{\sin}^{i,\tau,f_c} \right)^2 \geq \frac{1}{\pi} \left(2 \frac{\lambda_{thresh} - c_{\lambda_0}}{c_\lambda a_{\text{sig}}^2} - c_{z^T P^{-1} z} \right), \quad (25)$$

or

$$\overline{\lambda}_{\text{LMP}} \geq \overline{\lambda}_{\text{LMP,tresh}}. \quad (26)$$

The left-hand side of the inequality can be evaluated independent of a_{sig}.

The test statistic in Equation (26) indicates, to a particular level of probability of false alarm, a signal is present. In the proposed application more information is required, namely that the correct signal has been detected. Because the signatures vary over i, τ, f_c,

$$\overline{\lambda}_{\text{LMP}}^{i,\tau,f_c}(\mathbf{y}) = \left(\mathbf{y}^T P^{-1} \mathbf{z}_{\cos}^{i,\tau,f_c} \right)^2 + \left(\mathbf{y}^T P^{-1} \mathbf{z}_{\sin}^{i,\tau,f_c} \right)^2. \quad (27)$$

From Equation (27) define $\eta_{\text{LMP,cos}}^{i,\tau,f_c}$ and $\eta_{\text{LMP,sin}}^{i,\tau,f_c}$ as the square of the correlations between the measurements $\mathbf{y}$ and the mode perturbation signatures with in-phase and quadrature carriers. The approach is to use $\overline{\lambda}_{\text{LMP}}^*$ both as a signal detector and as an optimization tool over i, τ, f_c, or

$$\overline{\lambda}_{\text{LMP}}^* = \max_{i,\tau,f_c} \left\{ \eta_{\text{LMP,cos}}^{i,\tau,f_c} + \eta_{\text{LMP,sin}}^{i,\tau,f_c} \right\}. \quad (28)$$

The test statistic in Equation (28) is a function of the i^{th} mode, Gold Code phase τ, and frequency f_c, but it is not a function of the carrier phase delay θ. These parameters are estimated by maximizing $\overline{\lambda}_{\text{LMP}}^{i,\tau,f_c}$, or

$$\hat{i}, \hat{\tau}, \hat{f_c} = \arg\max \left\{ \eta_{\text{LMP,cos}}^{i,\tau,f_c} + \eta_{\text{LMP,sin}}^{i,\tau,f_c} \right\}. \quad (29)$$

The LMP statistic in Equation (28) was developed by assuming that a_{sig} is known. But in practice, a_{sig} is estimated. Thus, the terms on the right-hand side of Equation (28) must be related to the estimator.

Consider the alternate hypothesis,

$$H_{1,\cos} : \mathbf{y} = a_{\text{sig}} \mathbf{z}_{\cos}^{i,\tau,f_c} + \mathbf{n}, \quad (30)$$

where Equation (30) differs from H_1, Equation (8), by the fact that the mode perturbation signature is expressed in terms of the in-phase ($\mathbf{z}_{\cos}^{i,\tau,f_c}$) signature replica. The likelihood for $H_{1,\cos}$ is written as:

$$p\left(\mathbf{y}|H_{1,\cos}\right) = \frac{1}{2\pi^{\frac{nm}{2}} |P|^{\frac{1}{2}}} \exp\left[-\frac{1}{2} \left(\mathbf{y} - a_{\text{sig}} \mathbf{z}_{\cos}^{i,\tau,f_c} \right)^T P^{-1} \left(\mathbf{y} - a_{\text{sig}} \mathbf{z}_{\cos}^{i,\tau,f_c} \right) \right]. \quad (31)$$

Assuming that the hypothesis $H_{1,\cos}$ is satisfied, an estimate of a_{sig} can be found by maximizing the likelihood $p\left(\mathbf{y}|H_{1,\cos}\right)$ given in Equation (31) or:

$$\hat{a}_{\text{sig}} = \arg\max_{a_{\text{sig}}} p\left(\mathbf{y}|H_{1,\cos}\right) = \min_{a_{\text{sig}}} \mathcal{L}\left[\mathbf{y}|H_{1,\cos}\right], \quad (32)$$

where $\mathcal{L}$ is defined as the log likelihood. Because the natural logarithm function is monotonically increasing, it can be used to simplify Equation (32):

$$\mathcal{L}^*\left[\mathbf{y}|H_{1,\cos}\right] = \min_{a_{\text{sig}}} \left[-\frac{1}{2} \left(\mathbf{y} - a_{\text{sig}} \mathbf{z}_{\cos}^{i,\tau,f_c} \right)^T P^{-1} \left(\mathbf{y} - a_{\text{sig}} \mathbf{z}_{\cos}^{i,\tau,f_c} \right) \right], \quad (33)$$

where $c_{\log} = \log\left(2\pi^{-\frac{m}{2}} |P|^{-\frac{1}{2}}\right)$ is a constant and can be removed from the optimization in Equation (33) with no loss in generality.

From Equation (33), the optimal maximum likelihood estimate of a_{sig} is:

$$\hat{a}_{\text{sig},H_{1,\cos}} = \frac{\mathbf{y}^T P^{-1} \mathbf{z}_{\cos}^{i,\tau,f_c}}{\left(\mathbf{z}_{\cos}^{i,\tau,f_c} \right)^T P^{-1} \mathbf{z}_{\cos}^{i,\tau,f_c}}. \quad (34)$$

Substituting Equation (34) into Equation (33) results in:

$$\overline{\mathcal{L}}\left[\mathbf{y}|H_{1,\cos}, \hat{a}_{\text{sig}}\right] = \frac{1}{2} \left(\mathbf{y}^T P^{-1} \mathbf{y} - \frac{\left[\mathbf{y}^T P^{-1} \mathbf{z}_{\cos}^{i,\tau,f_c} \right]^2}{(\mathbf{z}_{\cos}^{i,\tau,f_c})^T P^{-1} \mathbf{z}_{\cos}^{i,\tau,f_c}} \right), \quad (35)$$

where $\overline{\mathcal{L}}\left[\mathbf{y}|H_{1,\cos}, \hat{a}_{\text{sig}}\right]$ is defined as the likelihood when the optimal value of the estimate of a_{sig} is used.

Equation (35) is very similar to $\eta_{\text{LMP,cos}}^{i,\tau,f_c}$ in Equation (28). as a LMP test statistic similar to Equation (28) to determine the transmitted signal parameters. Noting that the $\mathbf{y}^T P^{-1} \mathbf{y}$ term in Equation (35) is not a function of a_{sig} or the optimization variables i, τ, and f_c, and

$$c_{\text{sig}}^{i,\tau,f_c} = \left(z_{\text{sig,cos}}^{i,\tau,f_c} \right)^T P^{-1} z_{\text{sig,cos}}^{i,\tau,f_c} \quad (36)$$

is known, the in-phase test statistic can be written as:

$$\eta_{\text{LMP,cos}}^{i,\tau,f_c} = \frac{1}{2} \left[\mathbf{y}^T P^{-1} \mathbf{z}_{\cos}^{i,\tau,f_c} \right]^2, \quad (37)$$

$$= \left\{ -\overline{\mathcal{L}}\left[\mathbf{y}|H_{1,\cos}, \hat{a}_{\text{sig}}\right] + \mathcal{L}\left[\mathbf{y}|H_0\right] \right\} c_{\text{sig}}^{i,\tau,f_c}, \quad (38)$$

where $\mathcal{L}\left[\mathbf{y}|H_0\right]$ is the likelihood for H_0 or $a_{\text{sig}} = 0$. Note that adding $\mathcal{L}\left[\mathbf{y}|H_0\right]$ to the negative value of $\overline{\mathcal{L}}\left[\mathbf{y}|H_{1,\cos}, \hat{a}_{\text{sig}}\right]$, does not modify the solution to the optimization problem over i, τ, and f_c.

Consider another hypothesis,

$$H_{1,\sin} : \mathbf{y} = a_{\text{sig}} \mathbf{z}_{\sin}^{i,\tau,f_c} + \mathbf{n}, \quad (39)$$

where Equation (39) differs from H_1, Equation (8), by the fact that the mode perturbation signature is expressed in terms of the quadrature ($\mathbf{z}_{\sin}^{i,\tau,f_c}$) signature replica. The same procedure can be used to show that:

$$\eta_{\text{LMP,sin}}^{i,\tau,f_c} = \left\{ -\overline{\mathcal{L}}\left[\mathbf{y}|H_{1,\sin}, \hat{a}_{\text{sig}}\right] + \mathcal{L}\left[\mathbf{y}|H_0\right] \right\} c_{\text{sin}}^{i,\tau,f_c}. \quad (40)$$

Substituting Equations (38) and (40) into Equation (28) produces the following optimization:

$$\hat{i}, \hat{\tau}, \hat{f_c} = \arg\max_{i,\tau,f_c} \left[\eta_{\text{LMP,cos}}^{i,\tau,f_c} + \eta_{\text{LMP,sin}}^{i,\tau,f_c} \right], \quad (41)$$

$$= \arg\max_{i,\tau,f_c} \left\{ 2 \cdot \mathcal{L}\left[\mathbf{y}|H_0\right] - \mathcal{L}\left[\mathbf{y}|H_{1,cos}, \hat{a}_{\text{sig}}\right] - \mathcal{L}\left[\mathbf{y}|H_{1,sin}, \hat{a}_{\text{sig}}\right] \right\} \quad (42)$$

where the constant $c_{\text{sig}}^{i,\tau,f_c}$ is removed from Equation (42) as it is inconsequential to the optimization.

With the proposed optimization of the test statistic in Equation (28), the likelihoods in Equations (37) and (40) are now related to the KF which is used to recursively estimate $\hat{a}_{\text{sig}}$.

It is proposed that the amplitude of the perturbation signature, a_{sig}, is estimated from noisy measurements using a model-based estimator. Consider the discrete time linear system:

$$\mathbf{x}_{k+1} = A_k \mathbf{x}_k + B_u \mathbf{u}_k + \mathbf{w}_k^x, \quad (43)$$

where $\mathbf{x}_k \in \mathbb{R}^{n_x}$ is the system state, $\mathbf{u}_k \in \mathbb{R}^{n_u}$ is the control input and $\mathbf{w}_k^x \in \mathbb{R}^{n_x}$ is zero-mean Gaussian process noise with covariance Q_k . Consider a full-state feedback control law with gain K based on Equation (5) where the objective of the controller is to make the system track a reference (that includes a mode perturbation signature or Gold Code).

The evolution of the nominal reference is expressed as a random walk described by matrix A_r and zero-mean Gaussian process noise $\mathbf{w}_k^r \in \mathbb{R}^{n_x,n_x}$ with covariance Q_k^r. Stacking $\mathbf{x}_k$, $\mathbf{r}_k$, and a_{sig} into a vector, the following system is derived:

$$\begin{bmatrix} \mathbf{x}_{k+1} \\ \mathbf{r}_{k+1} \\ a_{\text{sig},k+1} \end{bmatrix} = \begin{bmatrix} A_k - B_u K & B_u K & B_u K t_z^r\left(z_{\text{sig}}^{i,\tau,f_c}\right) \\ \mathbf{0} & A_r & \mathbf{0} \\ \mathbf{0} & \mathbf{0} & 1 \end{bmatrix} \begin{bmatrix} \mathbf{x}_k \\ \mathbf{r}_k \\ a_{\text{sig},k} \end{bmatrix} + \overline{\mathbf{w}}_{\mathbf{k}}, \quad (44)$$

where $\mathbf{0}$ are matrices of zeros of appropriate dimensions and $\overline{\mathbf{w}}_k = \begin{bmatrix} \mathbf{w}_k^x & \mathbf{w}_k^r & w_k^a \end{bmatrix}^T$ is a stacked vector containing the process noise for the state, the reference, as well as the process noise perturbing the amplitude of the perturbation signature, w_k^a. Let $\overline{\mathbf{x}}_k = \begin{bmatrix} \mathbf{x}_k & \mathbf{r}_k & a_{\text{sig}} \end{bmatrix}^T$ be the stacked state vector used in Equation (44). It should be noted that a_{sig} is added to the system state in order to relate the likelihoods in Equations (37) and (40) to the KF. In the measurement output equation, $\mathbf{v}_k$ is zero-mean Gaussian noise with covariance R_k added to $\mathbf{x}$.

The next step is to relate the KF estimate of the system from Equation (44) to the LMP detector. The form of the LMP in Equation (28) is related to the KF by considering the negative log likelihood cost conditioned on measurements up to sample k. The joint probability distribution of the measurements up to k conditioned on the hypothesis $H_{\{\cdot\}}$, where $H_{\{\cdot\}}$ is either H_0 (the signal is absent), $H_{1,\cos}$ (the in-phase component of the signal is present), or $H_{1,\sin}$ (the quadrature component of the signal is present), can be written as:

$$p\left[\mathbf{Y}^k | H_{\{\cdot\}}\right] = p\left[\mathbf{y}_k, \mathbf{Y}^{k-1} | H_{\{\cdot\}}\right] \quad (45)$$

The distribution can be furthered simplified using Bayes' Rule:

$$p\left[\mathbf{Y}^k | H_{\{\cdot\}}\right] = p\left[\mathbf{y}_k | \mathbf{Y}^{k-1}, H_{\{\cdot\}}\right] p\left[\mathbf{Y}^{k-1} | H_{\{\cdot\}}\right] = \prod_{j=1}^{k} p\left[\mathbf{y}_j | \mathbf{Y}^{j-1}, H_{\{\cdot\}}\right]. \quad (46)$$

Because a KF is used to estimate the augmented state, $\overline{\mathbf{x}}_k$, the distributions in Equation (46) are Gaussian, or

$$p\left[\mathbf{y}_j | \mathbf{Y}^{j-1}, H_{\{\cdot\}}\right] = \mathcal{N}\left[\mathbf{y}_j - \hat{\mathbf{y}}_j; 0, S_j | H_{\{\cdot\}}\right] = p\left[\nu_i | H_{\{\cdot\}}\right], \quad (47)$$

where $\nu_j = \mathbf{y}_j - \hat{\mathbf{y}}_j$ is the estimator's innovation at sample j, and S_j is its covariance. Substituting Equation (47) into Equation (46) equals:

$$p\left[\mathbf{Y}^k | H_{\{\cdot\}}\right] = \prod_{j=1}^{k} p\left[\nu_j | H_{\{\cdot\}}\right] \quad (48)$$

Since $p\left[\mathbf{Y}^k | H_{\{\cdot\}}\right]$ is conditioned on the system model, Equation (48), is actually the likelihood of the measurement sequence. In other words, $p\left[\mathbf{Y}^k | H_{\{\cdot\}}\right]$ is equivalent to the likelihood function derived in Equation (35) or Equation (40). The negative log likelihood function, Equation (48), is also related to the KF innovations:

$$\mathcal{L}_{KF}\left(\mathbf{Y}^k | H_{\{\cdot\}}\right) = -\log p\left[\mathbf{Y}^k | H_{\{\cdot\}}\right] = \left[\frac{1}{2}\sum_{j=0}^{k} \nu_j^T S_j^{-1} \nu_j\right]_{H_{\{\cdot\}}}. \quad (49)$$

The log likelihood function for the KF for each hypothesis is the sum of the innovations up through sample k conditioned on the hypothesis $H_{\{\cdot\}}$ [12]. Since $\mathcal{L}\left(\mathbf{Y}^k | H_{\{\cdot\}}\right)$ is the likelihood function of the KF, the following substitutions can be made in Equations (38) and (40):

$$\mathcal{L}\left[\mathbf{y} | H_{\{\cdot\}}, \hat{a}_{\text{sig}}\right] = \mathcal{L}_{KF}\left(\mathbf{Y}^k | H_{\{\cdot\}}\right), \quad (50)$$

where $\hat{a}_{\text{sig}} = 0$ for H_0. The expressions in Equation (50) can be rewritten in terms of the KF innovations Equation (49) yielding:

$$\mathcal{L}\left[\mathbf{y} | H_{\{\cdot\}}, \hat{a}_{\text{sig}}\right] = \left[\frac{1}{2}\sum_{j=0}^{k} \nu_j^T S_j^{-1} \nu_j\right]_{H_{\{\cdot\}}} \quad (51)$$

It is now possible to relate the KF innovations to the original LMP statistic in Equation (27) and the associated optimization problem in Equation (28). Equation (51) can be substituted into Equation (42) to rewrite the signal detection optimization problem over i, τ, and f_c in terms of the KF innovations:

$$\hat{i}, \hat{\tau}, \hat{f}_c = \max_{i,\tau,f_c} \left\{ 2 \cdot \left[\frac{1}{2}\sum_{j=0}^{k} \nu_j^T S_j^{-1} \nu_j\right]_{H_0} - \left[\frac{1}{2}\sum_{j=0}^{k} \nu_j^T S_j^{-1} \nu_j\right]_{H_{1,\cos}} - \left[\frac{1}{2}\sum_{j=0}^{k} \nu_j^T S_j^{-1} \nu_j\right]_{H_{1,\sin}} \right\}. \quad (52)$$

In summary, for each i^{th} mode, τ Gold Code phase, and f_c carrier frequency, the locally most powerful test statistic in Equation (52) requires the evaluation of:

1) A KF under hypothesis H_0 that assumes no perturbation signature is present, $a_{\text{sig}} = 0$.
2) A KF under the hypothesis, $H_{1,\cos}$, that there is a perturbation signature present, with an in-phase carrier, $\cos(\cdot)$, that has the form $t_z^r\left(z_{\cos}^{i,\tau,f_c}\right)$.
3) A KF under the hypothesis, $H_{1,\cos}$, that there is a perturbation signature present, with a quadrature carrier, $\sin(\cdot)$, that has the form $t_z^r\left(z_{\sin}^{i,\tau,f_c}\right)$.

The values of i, τ, and f_c which maximize Equation (52) are declared under the LMP test as the detected parameters.

IV. Numerical Examples

The mode detection method based on the Neyman-Pearson locally most powerful statistic is numerically evaluated in this section using a linear system with linear output equations and a 2D linear model with nonlinear radar-like output equations. Because of its optimality for linear systems with Gaussian noise and well known equations, the discrete time KF [12] is used for state estimation in the linear example while the SPF is used for the nonlinear example [13].

A. Two State Linear Model with a Linear Output Equation

The dynamics of motion in one dimension are modeled using a linear point mass model to describe the motion in an inertial plane, resulting in:

$$\mathbf{x}_{k+1} = \begin{bmatrix} 1 & T \\ 0 & 1 \end{bmatrix} \mathbf{x}_k + \begin{bmatrix} 0 \\ T \end{bmatrix} u_k + \mathbf{w}_k, \quad (53)$$

where the state, $\mathbf{x}_k = [x_k, \dot{x}_k] \in \mathbb{R}^2$, contains the position and velocity of the vehicle in the x direction, $\mathbf{w}_k$ is zero-mean Gaussian process noise with covariance Q, and T is the sampling time. The controller in Equation (5) is a full state feedback controller, given as $u_k = K(-\mathbf{x}_k + \overline{\mathbf{r}}_k)$, is used for tracking the reference $\overline{\mathbf{r}}_k$.

TABLE I
OPERATING MODES AND CORRESPONDING MODE SIGNATURES WITH $n_\rho = 31$.

Mode	Behavior	Signature
1	A	[1100001010111001011011000011011]
2	B	[1100100001011101110111001110100]
3	C	[1010110110110010111101110101010]

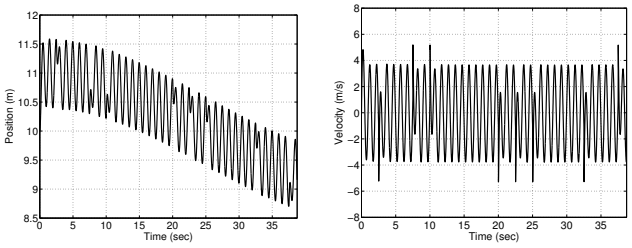

(a) (b)

Fig. 2. The response of the two state linear model to the combined position reference.

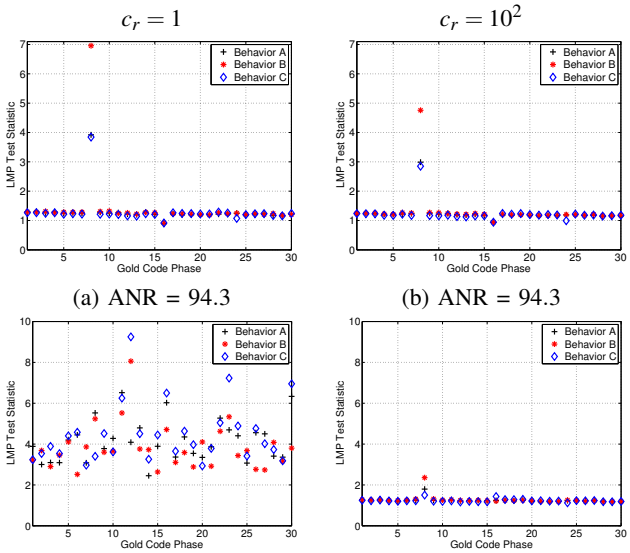

(a) ANR = 94.3 (b) ANR = 94.3

(c) ANR = 48.3 (d) ANR = 48.3

Fig. 3. Each row depicts the evaluation of the LMP test statistic for the two ANRs in decibels: 1) 94.3, and 2) 48.3 (from the top). The columns correspond to the LMP evaluation in which the KF measurement noise covariance is multiplied by $c_r = \left[1, 10^2\right]$.

The position trajectory of the simplified vehicle motion, is described by three operating modes: 1) behavior A, 2) behavior B, and 3) behavior C. These modes are defined with the signatures (Gold Codes) shown in Table I and implemented using BPSK [10]. Since the mode perturbation signature is embedded in the position reference, its derivative must be embedded in the tracking reference. Therefore, the function which maps from the scalar mode perturbation signature z^i_{sig} to the perturbation reference $\mathbf{r}^i_{\text{sig}}$ has the following form:

$$\mathbf{r}^i_{\text{sig},k} = a_{\text{sig}} \begin{bmatrix} z^i_{\text{sig},k} \\ \frac{d}{dt} z^i_{\text{sig},k} \end{bmatrix}. \tag{54}$$

The closed-loop response of the linear system to a combined position reference is shown in Figure 2.

The output equation is scalar with the form:

$$y_k = C\mathbf{x}_k + v_k = \begin{bmatrix} 1 & 0 \end{bmatrix} \mathbf{x}_k + v_k. \tag{55}$$

where v_k is zero-mean Gaussian noise with covariance R_k.

1) Kalman Filter Setup and Tuning: In the LMP, the KF uses replicas of the perturbation signatures as known inputs and estimates the system's nominal reference, $\hat{\mathbf{r}}_k$, and perturbation signature amplitude, $\hat{a}_{\text{sig}}$. An augmented state vector is defined composed of the $\mathbf{x}$, $\mathbf{r}$, and a_{sig}. The system has a full-state linear feedback controller gain, K. The carrier frequency of the carrier f_c is known and therefore dropped from the notation, while the frequency offset f_d is not considered here as its uncertainty is small for the system in this example.

The output equation of the system is linear and has the position as the sole measurement with Gaussian noise v_k with covariance R_k.

Tuning the elements of the diagonal process covariance matrix, $\overline{Q}_k$, is important for the optimal performance of the KF. The process noise covariance matrices found to result in the best estimates for the KFs corresponding to the hypotheses that no signal is present, $\overline{Q}^{H_0}_k$, and a mode perturbation signature is present, $\overline{Q}^{H_1}_k$ are:

$$\overline{Q}^{H_0}_k = \text{diag}\left(\left[10^{-3},\ 10^{+2},\ 10^{-1},\ 10^{+1}\right]\right). \tag{56}$$

$$\overline{Q}^{H_1}_k = \text{diag}\left(\left[10^{-3},\ 10^{+2},\ 10^{-1},\ 10^{+1},\ 10^{0}\right]\right). \tag{57}$$

In this investigation, the amplitude-to-noise ratio (ANR) is defined as:

$$\text{ANR} = \frac{a^2_{\text{sig}}}{2R_{\max}}, \tag{58}$$

where $R_{\max}$ is maximum element of the measurement noise covariance matrix, or $R_{\max} = \max R(l,l)$, for $l = 1, \ldots, n_y$. The relationship between the ANR and the signal-to-noise ratio (SNR) commonly used in detection is: $\text{SNR} = \text{ANR} \times k_{\max}$, where $k_{\max}$ is the number of measurement samples considered or estimation horizon [9]. The ANR was defined independent of the estimation horizon in order to isolate its influence on the performance of the algorithm.

The measurement noise covariance matrix can be tuned to reduce the effects of measurement noise and increase the detection parameter separation in the LMP. In this one dimensional example, increasing the KF measurement noise covariance leads to the estimator which behaves as a low-pass filter by reducing the Kalman Gain [14]. Figure 3 shows the evaluation of the LMP test statistic when the KF measurement noise covariance is $R = c_r \cdot R_0$ where $c_r = \left[1, 10^2\right]$ and R_0 is the covariance matrix for each ANR value (the frequency of the position reference is 0.10 Hz). The figures shows that decreasing the bandwidth of the estimator reduces the value of the LMP test statistic for signals with the incorrect parameters. For the figures with ANR of 48.3, it can be seen that if the measurement noise covariance is not multiplied by a factor detection is difficult. An ANR ≤ 48.3 requires that the KF measurement covariance is increased by a factor of $c_r = 10^2$ for robust detection parameter separation. Increasing the measurement noise covariance allows the detector to perform better by reducing the test statistic value for the incorrect parameters. For this example, the best tradeoff is found when KF measurement noise covariance is multiplied by a factor of 10^2 as shown in Figure 3 as a larger multiplication factor reduces the bandwidth of the estimator excessively compromising performance.

2) Monte Carlo Simulations: This section compares the results for the optimal detection method using Monte Carlo methods. Simulations were repeated for a total of 50 trials with Gaussian process and

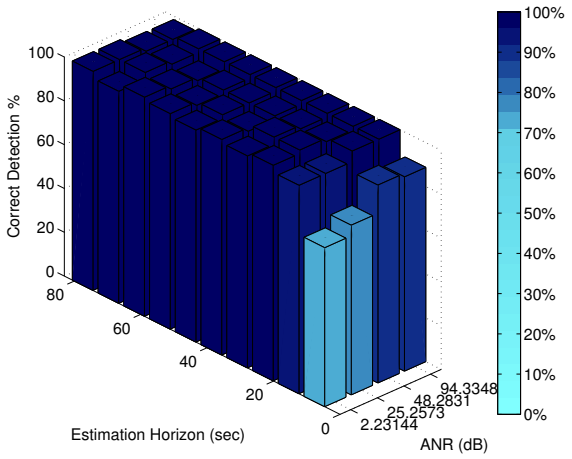

Fig. 4. Correct mode detection percentage for the LMP detector with a signature amplitude of $a_{\text{sig}} = 0.5$ tracking a reference frequency of 0.01 Hz.

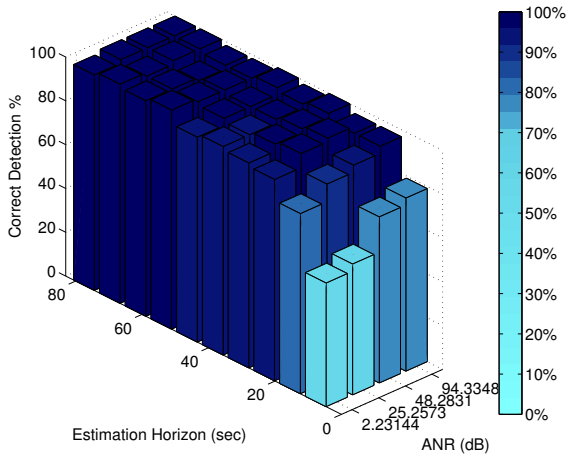

Fig. 5. Correct mode detection percentage for the LMP detector with a signature amplitude of $a_{\text{sig}} = 0.5$ tracking a reference frequency of 0.10 Hz.

measurement noise in order to obtain meaningful simulation statistics. In order to incorporate realistic maneuvers, the system tracked sinusoidal references with amplitude $a_r = 10$ at frequencies, f_r: 1) 0.01 Hz, 2) 0.10 Hz, and 3) 1.00 Hz. Four ANRs in decibels were also considered: 1) 2.2, 2) 25.3, 3) 48.3, and 4) 94.3. The performance of the detector was measured by considering the percentage of times the correct parameter (i and τ) were detected.

Figure 4 shows the performance of the LMP detector, Equation (52), with the system tracking a reference of 0.01 Hz. As would be expected, the performance of the detector improves as the estimation horizon and ANR increase. It can be seen that even for $ANR = 2.23$ acceptable performance of about 80% can be achieved if the estimation horizon is extended beyond 40 seconds. Figure 5 shows how increasing the frequency of the tracking reference to 0.10 Hz affects detection. The percentage performance is primarily not effected by this increase in the reference frequency in areas of large estimation horizon (> 40 seconds) and ANR (> 48.3). Most of the degradation in performance occurs for low ANRs. However, a tracking reference with frequency of 1.00 Hz deteriorates the performance of the detector. This effect is evident when Figure 6 is compared to Figures 4 and 5. For this condition, the nominal reference and the mode signature share the same frequency ($f_c = f_r = 1.0$ Hz) decreasing the performance of the LMP detector. However, as Figure 6 shows that a detection rate higher than 90% is attainable if the estimation horizon is large (> 60 seconds) and the ANR is large (≥ 94.3). Figures 4, 5, and 6 have sufficient information to select an estimation horizon and ANR and predict a rate of correct parameter detection.

B. Four State Linear Model with Nonlinear Radar-Like Equations

Motion in two dimensions is described by the following linear discrete time model:

$$\mathbf{x_{k+1}} = \begin{bmatrix} 1 & T & 0 & 0 \\ 0 & 1 & 0 & 0 \\ 0 & 0 & 1 & T \\ 0 & 0 & 0 & 1 \end{bmatrix} \mathbf{x_k} + \begin{bmatrix} 0 & 0 \\ T & 0 \\ 0 & 0 \\ 0 & T \end{bmatrix} \overline{\mathbf{u}}_k^i + \mathbf{w}_k, \qquad (59)$$

where the state, $\mathbf{x}_k$ is composed of the position and velocity along the x-axis and the position and its derivative along the y-axis, or $\mathbf{x}_k = [x_k \;\; \dot{x}_k \;\; y_k \;\; \dot{y}_k]^T \in \mathbb{R}^4$. The control input has components for each axis, $\overline{\mathbf{u}}_k^i = \left[u_k^{x,i} \;\; u_k^{y,i}\right]^T \in \mathbb{R}^2$, and is calculated using full-state feedback (see

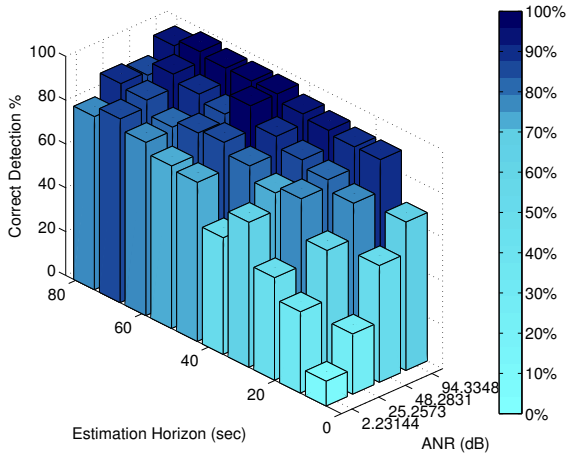

Fig. 6. Correct mode detection percentage for the LMP detector with a signature amplitude of $a_{\text{sig}} = 0.5$ tracking a reference frequency of 1.00 Hz.

Equation(5)).

The nonlinear output equations are composed of radar-like measurements: the range, κ_k, and an angle, χ_k, relative to the x-axis. The nonlinear measurement equations are the following:

$$\begin{bmatrix} \kappa_k \\ \chi_k \end{bmatrix} = \begin{bmatrix} \sqrt{x_k^2 + y_k^2} \\ \tan^{-1}\left(\frac{y_k}{x_k}\right) \end{bmatrix} + \mathbf{v}_k, \qquad (60)$$

where $\mathbf{v}_k$ is zero-mean white Gaussian measurement noise with covariance R_k.

1) Sigma Point Filter Setup and Tuning: In this example, the setup of the SPF is similar to the one described for the KF in the linear example, the only differences coming from the fact that motion in the y-axis must be considered resulting in an augmented state with larger dimensions. The nonlinear output equations used by the estimator are the same as the ones shown in Equation (60).

Although there is not a single best way to tune the estimator, simulation studies showed that it is most effective to start by minimizing the error in the velocity elements of the reference in both the x and

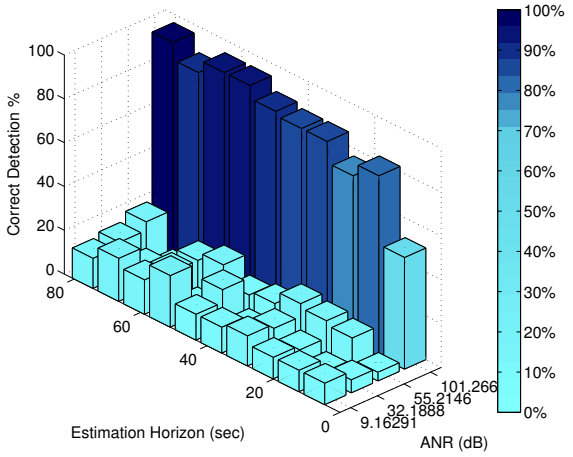

Fig. 7. Correct mode detection percentage for the LMP detector for the nonlinear example with $a_{\text{sig}} = 0.5$ and $f_r = 0.01$ Hz.

y directions and then to continue with the other elements. Therefore, the corresponding elements in the process covariance were tuned until the accuracy of the reference velocity estimate was maximized. As the elements in the covariance corresponding to the reference velocity were tuned, the reference position elements were also adjusted. The process covariance matrices found to produce the best estimates for the SPF in terms of maximizing the value of the test statistic for the correct parameters under hypothesis H_0 were the following:

$$\overline{Q}_k^{H_0} = \text{diag}\left(\left[10^{-1}, 10^{-3}, 10^{-1}, 10^{-3}, 10^{-1}, 10^{+4}, 10^{-1}, 10^{+4}\right]\right), \tag{61}$$

where $\overline{Q}_k^{H_0}$ is the SPF process noise covariance for the hypothesis that no signal is present, H_0, and

$$\overline{Q}_k^{H_1} = \text{diag}\left(\left[10^{-1}, 10^{+2}, 10^{-1}, 10^{+1}, 10^{-2}, 10^{+2}, 10^{+2}, 10^{+3}, 10^{-1}, 10^{0}\right]\right), \tag{62}$$

where $\overline{Q}_k^{H_1}$ is the SPF process noise covariance for the hypothesis that a signal is present with either with a cosine or sine carrier.

2) Monte Carlo Simulations: In the simulations, the radar sensor was located at the origin of an $x-y$ coordinate system while the motion of the vehicle started at the coordinates $(70, -20)$ with an initial speed of zero for both directions. The trajectory of the vehicle tracking a reference with amplitude $a_r = 10$ and frequency of $f_r = 0.01$ Hz and a amplitude of $a_{\text{sig}} = 0.5$. As with the linear numerical example, the simulations were repeated 50 trials with Gaussian process and measurement noise. The ANRs pairs in dBs for the angle and range measurements respectively were: 1) 9.2, 37.1, 2) 32.2, 60.2, 3) 55.2, 83.2, and 4) 101.3, 129.2.

The Monte Carlo simulations results in Figure 7 show that the performance of the LMP detector dropped off significantly for the ANR pair of less than 101.3 and 129.2 dBs. Figure 7 shows the simulation results, for an ANR= 101.3 the relationship between the estimation horizon and the performance is similar to the one seen in the simpler linear example (the ANR axis in the figure corresponds to the angle). However, the performance degrades quickly when the ANR is lowered to 55.2 and 83.2 dBs. Although not shown, the performance of the LMP degrades as the frequency of the reference increases. This nonlinear example is shown to demonstrate the applicability of the LMP detector to a nonlinear system. A more detailed analysis and simulations of the application of the LMP detector to a nonlinear system can be found in [15].

V. Summary

The problem of receiving information using movements instead of direct radio communication was investigated. The motivation of using a motion-based communication protocol was to establish a non-traditional method of exchanging information for situations in which radio communication is prohibited or faults have occurred. A hybrid system model was formulated under the assumption that the behavior can be described by a finite set of operating modes. Each mode consists of a model that describes the vehicle's dynamics as well as a mode perturbation signature. The signatures were designed as Gold codes since they are differentiable from noise and have favorable correlation properties. A locally most powerful detector was derived that uses principles from detection and estimation theory to derive an optimal test statistic. The LMP test statistic is evaluated using the KF innovations. Monte Carlo simulations of a one dimensional linear model and a two dimensional model with nonlinear radar-like measurements were presented.

Simulations showed the detection performance, defined as the percentage of times the correct mode perturbation signature parameters are detected, is a function of the estimation horizon and the ANR. The results also showed that as the frequency of the reference increases and is near the frequency of the mode perturbation signature, the performance of the detector degrades. In the linear example, it was shown that the proper tuning of the measurement noise covariance can significantly affect performance. The numerical example of a system with nonlinear radar-like measurement equations showed the applicability of the LMP detector to a nonlinear system.

References

[1] A. Richards, J. Bellingham, M. Tillerson, and J. How, "Co-ordination and control of multiple UAV's," in *Proc. of the AIAA Guidance, Navigation, and Control Conference*, August 2002.
[2] J. Ousingsawat and M. Campbell, "Multiple team tasking for cooperative estimation," in *Proc. AIAA Guid., Nav., and Cont. Conf.*, August 2004.
[3] Y. Liu, K. Passino, and M. Polycarpou, "Stability analysis of M-dimensional swarms with a fixed communication topology," *IEEE Transactions on Automatic Control*, vol. 48, pp. 76–95, January 2003.
[4] Y. Liu, K. Passino, and M. Polycarpou, "Stability analysis of one-dimensional asynchronous swarms," *IEEE Transactions on Automatic Control*, vol. 48, pp. 1848–1854, October 2003.
[5] V. Gazi and K. Passino, "Stability analysis of swarms," *IEEE Transactions on Automatic Control*, vol. 48, pp. 692–697, April 2003.
[6] J. Fax and R. Murray, "Information flow and cooperative control of vehicle formations," *IEEE T. A. Co.*, vol. 49, pp. 1465–1476, Sept. 2004.
[7] P. Otanez and M. Campbell, "Mode estimation switching using perburation signatures for hybrid multi-vehicle systems," in *Proc. of the AIAA Guidance, Navigation, and Control Conference*, August 2005.
[8] P. Otanez and M. Campbell, "Hybrid cooperative reconnaissance without communication," in *Proc. IEEE Conf. on Dec. and Cont.*, Dec. 2005.
[9] H. V. Poor, *An Intro. to Signal Det. and Est.* Springer-Verlag, 1994.
[10] R. L. Peterson, R. E. Ziemer, and D. E. Borth, *Introduction to Spread Spectrum Communications*. Prentice Hall, 1995.
[11] R. Gold, "Optimal binary sequences for spread spectrum multiplexing," *IEEE Trans. on Inf. Theory*, vol. 13, no. 4, pp. 619–621, 1967.
[12] Y. Bar-Shalom, X. R. Li, and T. Kirubarajan, *Estimation with Applications to Tracking and Navigation*. John Wiley and Sons, Inc., 2001.
[13] S. Julier, J. Uhlmann, and H. Durrant-Whyte, "A new method for the nonlinear transformation of means and covariances in filters and estimators," *IEEE Trans. Auto. Cont.*, vol. 45, no. 3, pp. 477–482, 2000.
[14] B. Ekstrand, "Poles and zeros of $\alpha-\beta$ and $\alpha-\beta-\gamma$ tracking filters," *IEE Proc. of Control Theory App.*, vol. 148, pp. 370–376, Sept. 2001.
[15] P. Otanez, *Hybrid Estimation for Control and Planning*. Ph.D. dissertation, Cornell University, November 2007.